

Solar-Wind Hybrid Power Generation System Optimization Using Superconducting Magnetic Energy Storage (SMES)

Saad Nemdili

Department of Electrotechnics
Faculty of Technology
Ferhat Abbas University Setif 1
Setif, Algeria
snemdili@yahoo.com

Ian Chanetsa Ngaru

Department of Electrotechnics
Faculty of Technology
Ferhat Abbas University Setif 1
Setif, Algeria
chanetsa11@gmail.com

Meriem Kerfa

Department of Electrotechnics
Faculty of Technology
Ferhat Abbas University Setif 1
Setif, Algeria
merymed17@gmail.com

Received: 3 August 2022 | Revised: 22 August 2022, 5 September 2022, and 10 September 2022 | Accepted: 11 September 2022

Abstract-This paper proposes a renewable energy hybrid power system that is based on photovoltaic (PV) and wind power generation and is equipped with Superconducting Magnetic Energy Storage (SMES). Wind and solar power generation are two of the most promising renewable power generation technologies. They are suitable for hybrid systems because they are environmentally friendly. However, like most renewable energy sources, they are characterized by high variability and discontinuity. They generate a fluctuating output voltage that damages the machines that operate on a stable supply. Therefore, the energy storage system SMES with the function to reduce output voltage fluctuation problems is introduced. SMES is found to be the most effective energy storage device as a result of its quick time response, high power density, and high energy conversion efficiency. In this paper, modeling of a hybrid system with SMES is built using MATLAB/Simulink. Blocks such as the wind model, PV model, and energy storage model are built separately before combining into a complete hybrid system with SMES. Varying wind speed and solar irradiance values are taken as the input parameters. The obtained results from the simulation reveal that a system with SMES is more reliable than a system without SMES.

Keywords-hybrid energy storage system; renewable energy; photovoltaic (PV) system; wind; power quality; Superconducting Magnetic Energy Storage (SMES)

I. INTRODUCTION

During the last decades, the exploitation of renewable energy resources has attracted considerable attention due to the negative impact on the environment and the increased cost of fossil fuels used in conventional power plants. Many renewable

energy sources, like solar, wind, hydro, and tidal can be exploited. Among them, solar and wind have the most rapid growth. Without any hazard emission of pollutants, energy conversion is made possible through wind and PV cells.

A hybrid system is more advantageous as an individual power generation system, even though it is not completely reliable. In case of a power outage or complete shutdown in one of the systems, the remaining one can still supply power. Hence, in the present study, solar and wind power generations are combined to create a hybrid power system. This system, consisting of two unpredictable energy sources, will produce fluctuating output energy and thus cannot ensure the minimum level of power continuity required by the load [1-3]. Combining the renewable hybrid system with batteries as a storage system, in order to increase the duration of energy autonomy, will make optimal use of the utilized renewable energy resources and this, in turn, can guarantee high supply reliability.

At present, multiple energy storage technologies are being developed and such examples include Flywheel Energy System (FES), Compressed Air Energy Storage (CAES), Battery Energy Storage System (BESS), Superconducting Magnetic Energy Storage (SMES) [4], and Phase-Change Materials (PCM). In this paper, a SMES is introduced into the hybrid wind and PV power generation system. The added energy storage will store energy during the low load demand period and help stabilize the system's generated output voltage.

Corresponding author: Saad Nemdili

II. MODELING OF THE HYBRID SYSTEM

A. Modeling of the PV System

In this project, we chose to use KC200GT PV module as a reference to develop the PV block model. The PV system was modeled and developed based on the equations from [5]. The parameters of the PV model are shown in Table I.

TABLE I. PV ARRAY PARAMETERS AT 250°C, 1000w/m²

Parameter	Value
I_{mp}	7.61 A
V_{mp}	26.3 V
I_{sc}	8.21 A
P_{max}	200.143 W
V_{oc}	32.9 V
K_v	-0.1230 V/K
K_i	0.0032 A/K
N_s	54
N_p	4

The PV power system model is made up of 3 subsystem blocks (Figures 1-3), which are:

- Photovoltaic Current (I_{pv})
- Saturation Current (I_o)
- Photovoltaic Current Output (I_m)

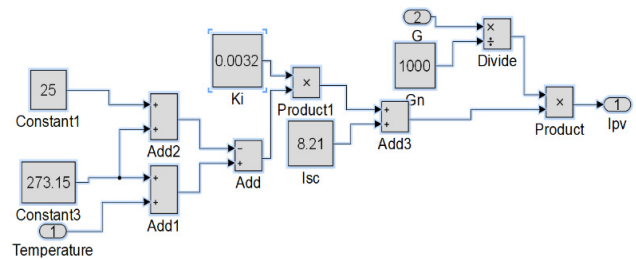


Fig. 1. Photovoltaic current block model.

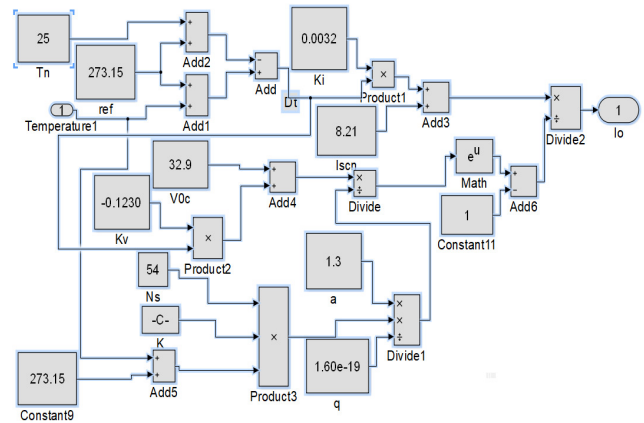


Fig. 2. Saturation current block model.

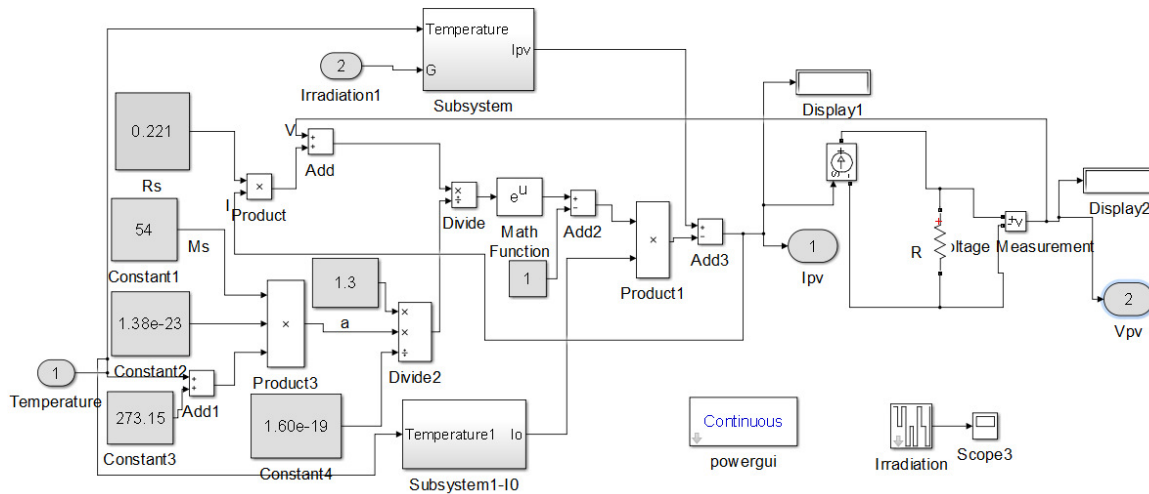


Fig. 3. Photovoltaic current output block model.

The parameters that affect the PV power system output are solar irradiance (G) and temperature (T). Both PV current and saturation current block models are connected in the PV current output block model, as illustrated in Figure 3.

B. Modeling of Wind Turbine Power System

The wind turbine power system consists of a wind turbine model and a Permanent Magnet Synchronous Machine (PMSM) block that was already available on the Simulink library of MATLAB. These permanent magnet machines are characterized by having large air gaps, which reduce the flux

linkage even in machines with multi-magnetic poles [6-8]. The static characteristics of wind turbines can be described by the relationship between the total power in the wind and the mechanical power of wind turbines [9-11].

The wind turbine model block is connected to a PMSM and a rectifier as shown in Figure 4. Varying wind speed is given as the input to the wind turbine and the output mechanical torque from the turbine is directed to the PMSM that converts mechanical energy into electrical energy. The three phase AC output from the PMSM is then sent to the rectifier where it is converted into the DC output.

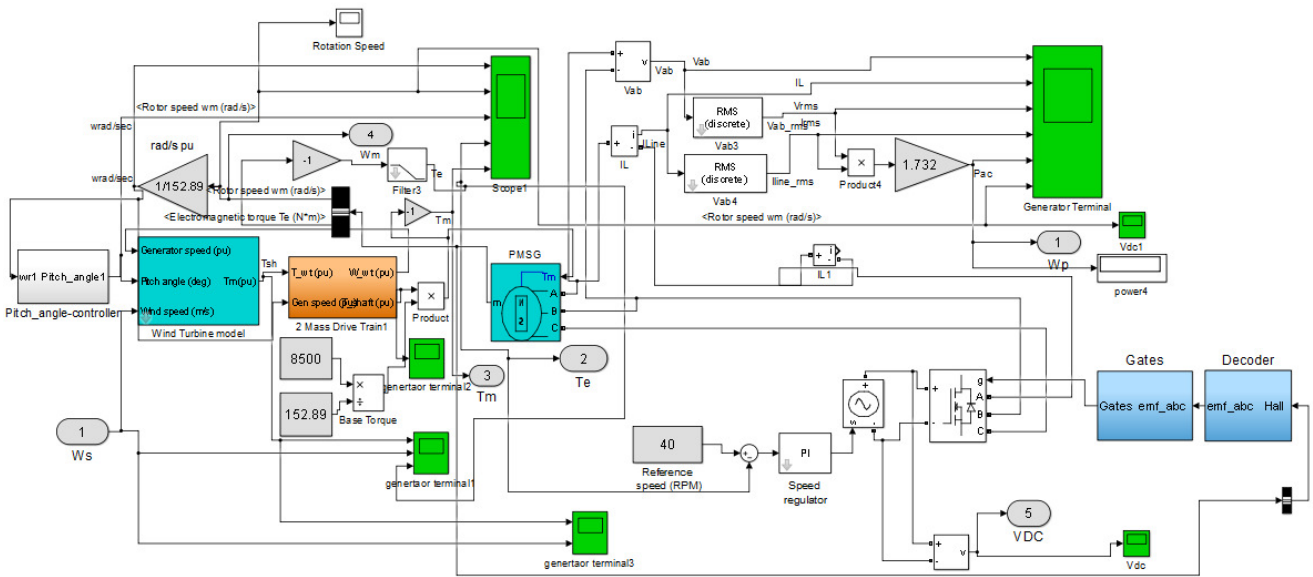


Fig. 4. Wind power system.

TABLE II. PARAMETERS OF THE PERMANENT MAGNET SYNCHRONOUS MACHINE BLOCK

Parameters	Value
Nominal mechanical output power (W)	8.5e3
Base power of the electrical generator (VA)	8.5e3/0.9
Base wind speed (m/s)	12
Maximum power at base wind speed (pu of nominal mechanical power)	0.8
Base rotational speed (kpu of base generator speed)	1

TABLE III. PARAMETERS OF THE WIND TURBINE BLOCK

Parameter	Value
Stator phase resistance R_s (ohm)	0.425
Inductance L_d (H)	0.000395
Flux linkage established by magnets (V.s)	0.433
Torque constant	5
Inertia J (kg.m ²)	0.1197
Friction factor F (N.m.s)	0.001189

The simulation of the wind power system is shown in Figure 4 and the parameters of the PMSM block and wind turbine model block are presented in Tables II and III respectively.

C. Modeling of the SMES System

A SMES device is a DC current device that stores energy in the magnetic field. The DC current flowing through a superconducting wire in a large magnet creates the magnetic field [12]. The basic operation of the SMES coil can be explained by the simplified electrical model in Figure 5.

In this model, the SMES coil is connected to the source and is loaded by three switches: S1, S2, and S3. Here, the coil is a dynamic storage system. Charging and discharging of the coil is maintained by a Power Conditioning System (PCS) which controls the switches independently by generating suitable control of a signal. The operation of the switches is described by the flowchart in Figure 6.

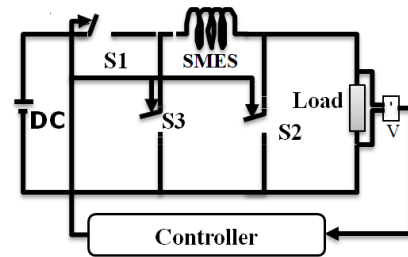


Fig. 5. Simplified equivalent circuit of the SMES coil.

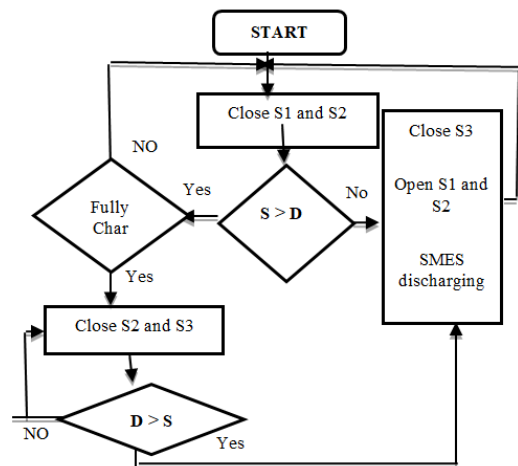


Fig. 6. Flowchart of charging-discharging involved in the SMES system.

1) First case

As seen in the circuit diagram, the superconducting coil is directly connected to the input voltage, whereas the load is through the aid of power electronics switches. The supply is denoted by "S" and the demand by "D". If $D < S$, S1 and S2 must be closed and switch S3 is open. This combination is used to charge the coil.

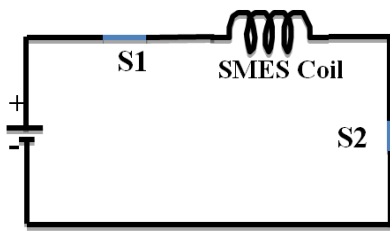


Fig. 7. Circuit of charging SMES coil.

2) Second Case

When switches S3 and S2 are closed and switch S1 is open, the coil will be in the steady storage condition.

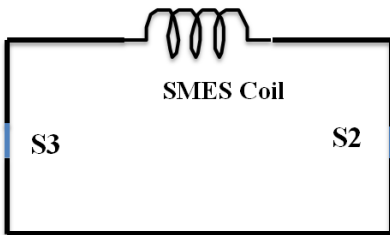


Fig. 8. Circuit of the steady storage case.

3) Third case

In this case, switches S1 and S2 are open and switch S3 is closed and the coil will be discharging.

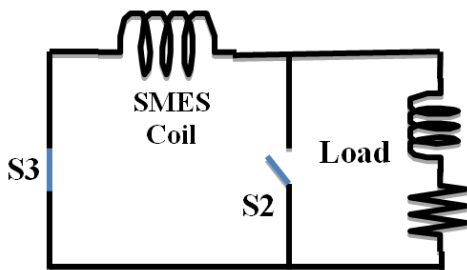


Fig. 9. Circuit of the case of discharging of the SMES coil.

D. Controller Circuit

An appropriate control system was required to control the charging and discharging sequence of the SMES. This was accomplished by using a PI controller-based DC-DC chopper as shown in Figure 10. It operates by constantly comparing the reference voltage with the feedback value of the controller. The error difference between these two will be added to the voltage output from the hybrid system [13]. This total output voltage will then be compared with the expected hybrid output voltage using a comparator. If the output of the hybrid system is less than the reference value, then the DC-DC chopper sends signal zero (0) to the switch, otherwise, a signal one (1) will be sent. Signal zero (0) indicates a switch open and SMES discharging, whereas signal one (1) indicates that the IGBT switch is closed and SMES is charging.

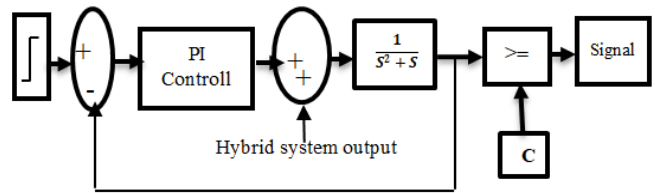


Fig. 10. DC-DC chopper controller block model.

III. SIMULATION CASE STUDIES

In this section, various case studies are been considered. In each case, the input solar irradiance and the wind speed were considered different. Hybrid system power characteristics, i.e. input solar irradiance and input wind speed, with and without SMES and SMES power characteristics are plotted for each case.

A. Simulation Results of the SMES System

Modeling of the charge-discharge circuit for the SMES is executed using MATLAB/Simulink. The circuit (Figure 14) is implemented for a purely resistive load. The parameters of the SMES model are shown in Table IV.

TABLE IV. SMES PARAMETERS

Parameter	Value
System frequency	50 Hz
Line reactor resistance	0.0015 Ω
DC-Link capacitance	1 F
Load resistance	1 Ω
Superconducting coil	0.008H
PID Controller Gain	KP =0.5, KI = 0.00001, KD= 1

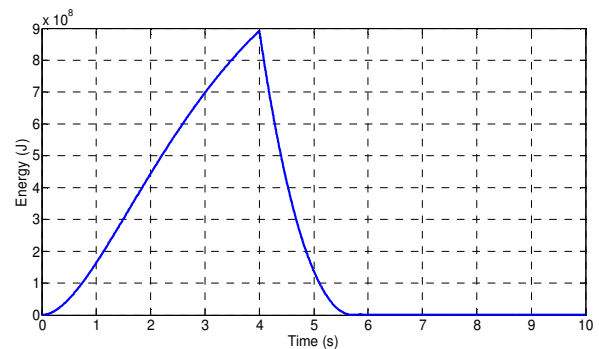


Fig. 11. Energy waveform during coil charging and discharging.

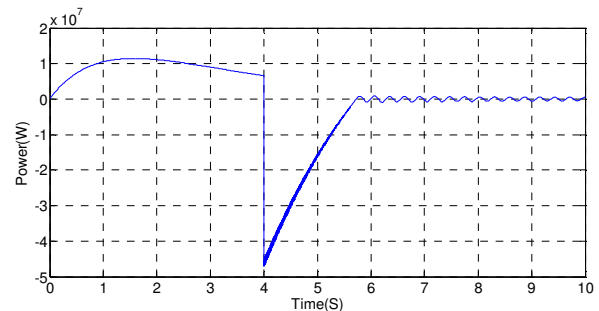


Fig. 12. Power waveform during coil charging and discharging.

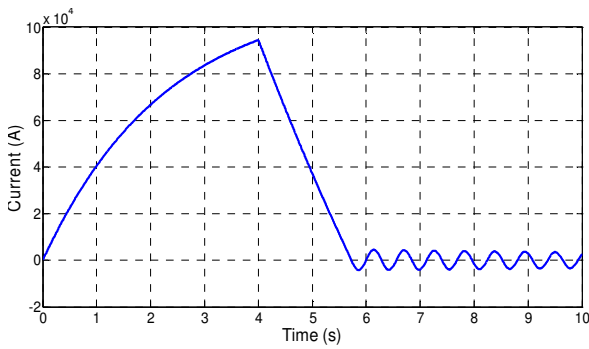


Fig. 13. Current waveform during coil charging and discharging.

From the results, it is evident that the SMES can store very high energy, around 1000MJ, whereas the power level is close to 12MW and the current increases until it reaches around 100kA. During the discharge of the coil, the power injection time is also very low (2s).

B. Simulation Results of the Hybrid System without SMES

The two renewable generator types are connected in series. Each generator produces a voltage output of 200V, so practically the output voltage was 400V. We simulated the hybrid system for 3 cases to see the influence of the intermittency of the wind and irradiation on the charging voltage. The system supplies an electrical load (R, L) with $R= 30\Omega$ and $L= 2H$.

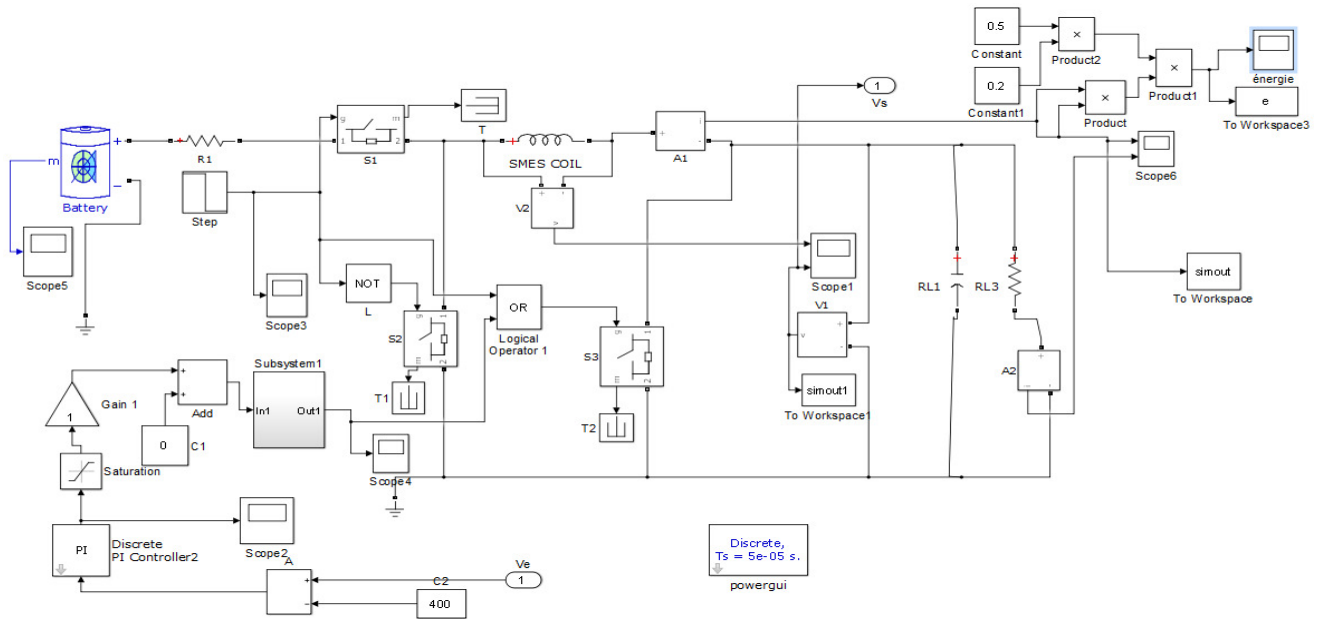


Fig. 14. SMES system block model.

- Case 1: Irradiation and wind speed are constant, $G= 1000w/m^2$, $V= 12m/s$. Figures 15, 16 show the Voltage rate and the power characteristic.

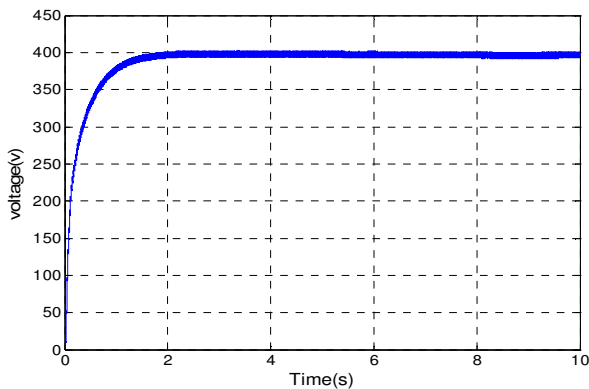


Fig. 15. Voltage rate.

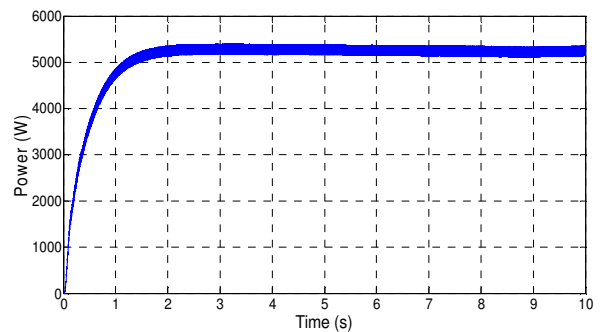


Fig. 16. Power characteristic.

- Case 2: The irradiation is of Step form and the wind speed remains constant. Figures 17, 18 show the Voltage rate and the power characteristic.

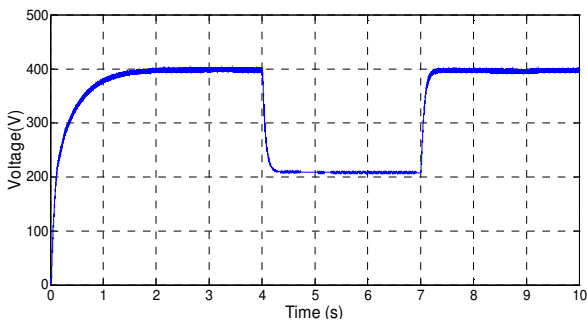


Fig. 17. Voltage rate.

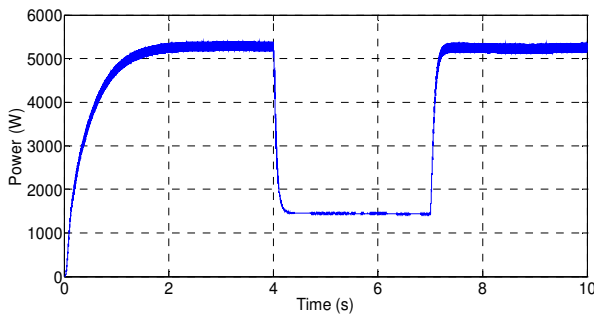


Fig. 18. Power characteristic.

- Case 3: Constant irradiation and step form wind speed. Figures 19, 20 show the Voltage rate and the power characteristic.

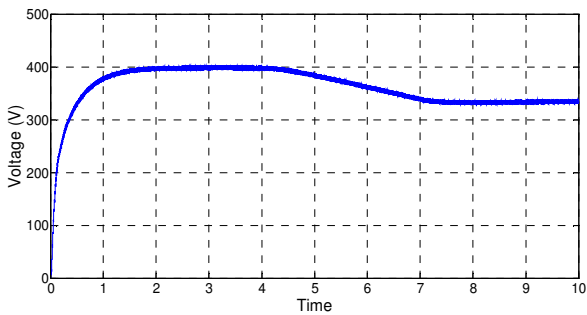


Fig. 19. Voltage rate.

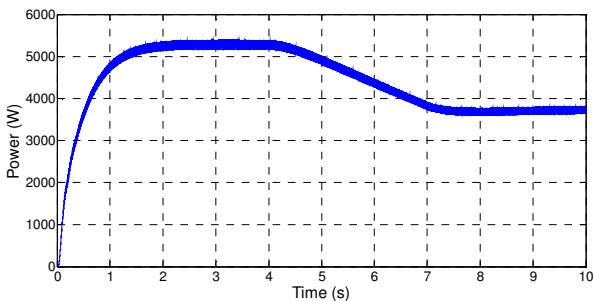


Fig. 20. Power characteristic.

From Figures 15-20, it is clear that when the wind or irradiation or both decrease, the load voltage decreases along with power.

C. Simulation of the Hybrid Wind-PV System with SMES

This study seeks to stabilize the voltage in the event of loss of one or both renewable generators. So, we integrated an energy storage system using a superconducting SMES coil, whose role is to intervene in the event of a voltage drop [14]. The simulation time of Figure 24 is 10s. We simulated the system for the case where the loss of the two generators from which the irradiation and wind speed have a step form. Figures 21-25 show the simulation results.

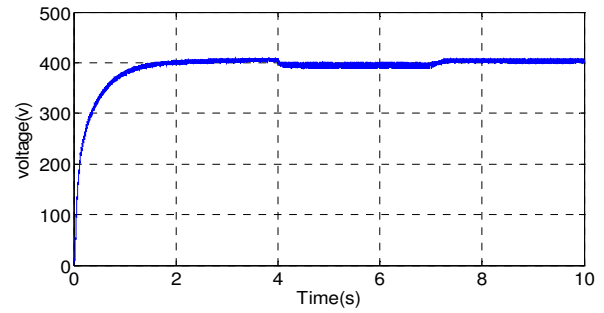


Fig. 21. Charge voltage curve with SMES.

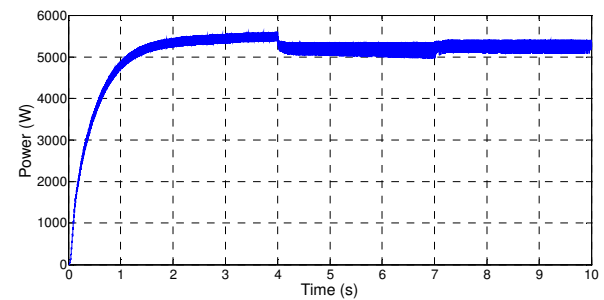


Fig. 22. Hybrid system power curve with SMES.

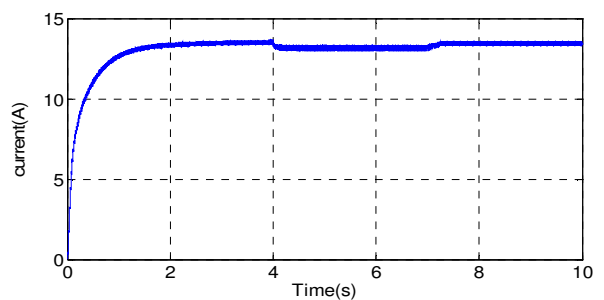


Fig. 23. Hybrid system charging current curve with SMES.

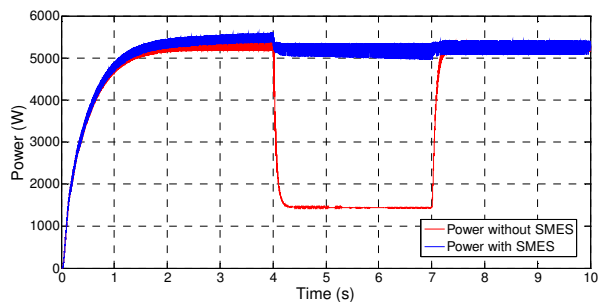


Fig. 24. Curve of Power with and without SMES.

According to Figure 21, during the period from 0s to 4s the voltage reached 400V. From 4s to 7s the two generators were lost and the voltage was restored thanks to the intervention of the SMES, which was able to keep it stable. Therefore, we can see the great contribution of SMES to the stability of the hybrid system. Figure 24 represents the comparison of the power with

and without SMES for the case of the loss of the two generators from 4s to 7s. We noticed that the power without SMES decreases when the wind and the irradiation decreased and on the other hand, with SMES, the power remains stable and is fixed at a value of 5200W.

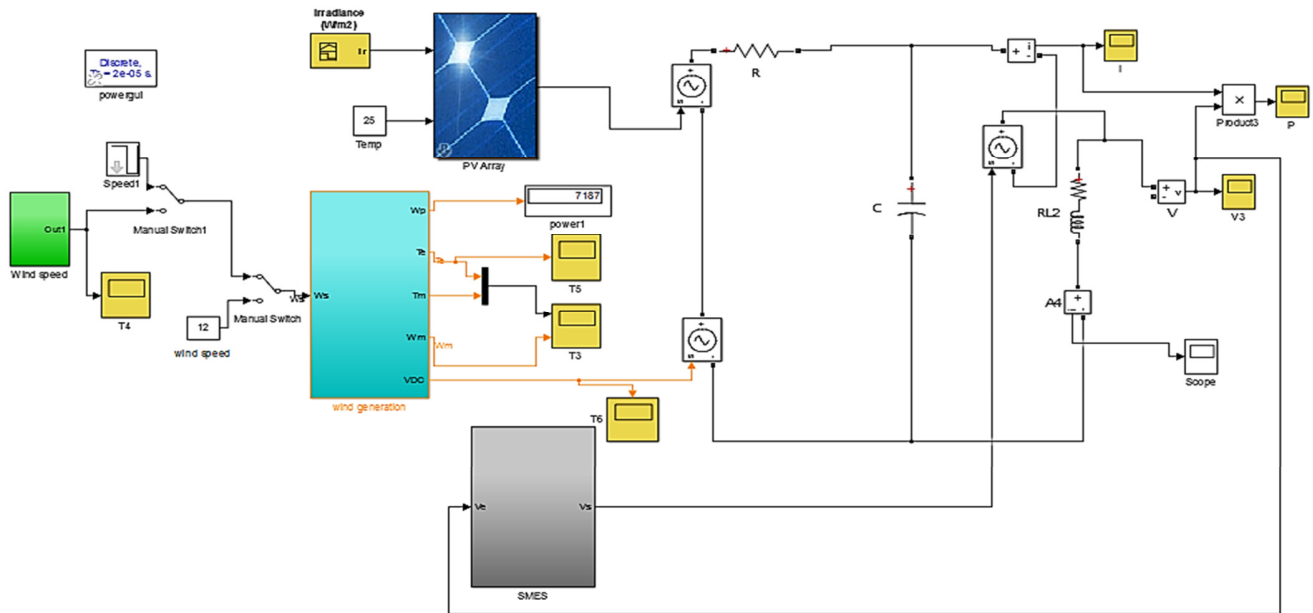


Fig. 25. Block diagram of the hybrid wind-PV system with SMES (the inside of sub-models is shown in Figures 1-4, 14).

D. Discussion

When both PV and wind generators are connected to the system, the load demand is met. If only one of the PV or the wind generators generates power, then the power demand of the system cannot be fulfilled since the two generators are connected in series to give an added output voltage. From the hybrid system power graph, it is seen that voltage drops when one generator is lost or disturbed making the system unstable. When the SMES is added to the system, it provides power with very fast response time, which ensures the constant output power of the hybrid system. This is clearly shown in the graph of the hybrid system power with and without SMES (Figure 24). Based on the simulation results, SMES technology can also be used on conventional generating systems for load leveling and spinning reverse.

IV. CONCLUSIONS

In this paper, a hybrid system that combines the wind and PV models has been developed, and the application of the energy storage system SMES is presented in the developed model. The overall hybrid system with and without SMES was tested with varying irradiation levels and wind speed for the PV model and the wind model to determine the function of SMES inside the hybrid system. Through the charging and discharging process of SMES during the simulation, the output voltage fluctuations caused by the intermittent energy sources in the power generation system were reduced. It has been seen from the simulation results that SMES can improve the quality of the

output fluctuations, and thus increase the reliability of the hybrid power system.

REFERENCES

- [1] A. Kumar, K. S. Sandhu, S. P. Jain, and P. Sharath Kumar, "Modeling and Control of Micro-Turbine Based Distributed Generation System," *International Journal of Circuits, Systems and Signal Processing*, vol. 2, no. 3, pp. 65–72, 2009.
- [2] A. Al-Shereiqi, A. Al-Hinai, M. Albadi, and R. Al-Abri, "Optimal Sizing of Hybrid Wind-Solar Power Systems to Suppress Output Fluctuation," *Energies*, vol. 14, no. 17, Jan. 2021, Art. No. 5377, <https://doi.org/10.3390/en14175377>.
- [3] A. Safaei, S. H. Hosseinian, and H. A. Abyaneh, "Enhancing the HVRT and LVRT Capabilities of DFIG-based Wind Turbine in an Islanded Microgrid," *Engineering, Technology & Applied Science Research*, vol. 7, no. 6, pp. 2118–2123, Dec. 2017, <https://doi.org/10.48084/etasr.1541>.
- [4] A. Zebar and L. Madani, "SFCL-SMES Control for Power System Transient Stability Enhancement Including SCIG-based Wind Generators," *Engineering, Technology & Applied Science Research*, vol. 10, no. 2, pp. 5477–5482, Apr. 2020, <https://doi.org/10.48084/etasr.3422>.
- [5] S. Sumathi, L. Ashok Kumar, and P. Surekha, *Solar PV and Wind Energy Conversion Systems*. Springer International Publishing, 2015.
- [6] P. Vas, *Electrical Machines and Drives: A Space-Vector Theory Approach*, 1st ed. Oxford, UK; New York, NY, USA: Clarendon Press, 1993.
- [7] T. J. E. Miller, *Brushless Permanent-Magnet and Reluctance Motor Drives*. Oxford, UK: Oxford University Press, 1989.
- [8] K. Okedu, "Wind Turbine Driven by Permanent Magnet Synchronous Generator," *The Pacific Journal of Science and Technology*, vol. 12, no. 2, pp. 168–175, Oct. 2011.

- [9] A. Manyonge, R. Manyala, F. Onyango, and J. Shichika, "Mathematical Modelling of Wind Turbine in a Wind Energy Conversion System: Power Coefficient Analysis," *Applied Mathematical Sciences*, vol. 6, no. 91, pp. 4527–4536, Jan. 2012.
- [10] Y. D. Song, B. Dhinakaran, and X. Y. Bao, "Variable speed control of wind turbines using nonlinear and adaptive algorithms," *Journal of Wind Engineering and Industrial Aerodynamics*, vol. 85, no. 3, pp. 293–308, Apr. 2000, [https://doi.org/10.1016/S0167-6105\(99\)00131-2](https://doi.org/10.1016/S0167-6105(99)00131-2).
- [11] A. Goudarzi and F. Ghayoor, "Modelling of Wind Turbine Power Curves (WTPCs) Based on the Sum of the Sine Functions and Improved version of Particle Swarm Optimization (IPSO)," in *2020 International SAUPEC/RobMech/PRASA Conference*, Cape Town, South Africa, Jan. 2020. <https://doi.org/10.1109/SAUPEC/RobMech/PRASA48453.2020.9041008>.
- [12] T. Ise, M. Kita, and A. Taguchi, "A hybrid energy storage with a SMES and secondary battery," *IEEE Transactions on Applied Superconductivity*, vol. 15, no. 2, pp. 1915–1918, Jun. 2005, <https://doi.org/10.1109/TASC.2005.849333>.
- [13] G. H. Kim *et al.*, "A novel HTS SMES application in combination with a permanent magnet synchronous generator type wind power generation system," *Physica C: Superconductivity and its Applications*, vol. 471, no. 21, pp. 1413–1418, Nov. 2011, <https://doi.org/10.1016/j.physc.2011.05.206>.
- [14] A. B. Lajimi, S. A. Gholamian, and M. Shahabi, "Modeling and Control of a DFIG-Based Wind Turbine During a Grid Voltage Drop," *Engineering, Technology & Applied Science Research*, vol. 1, no. 5, pp. 121–125, Oct. 2011, <https://doi.org/10.48084/etasr.60>.